

# Contour interpolation revealed by a dot localization paradigm

Sharon E. Guttman\*, Philip J. Kellman

*University of California, Los Angeles, USA*

Received 12 August 2003; received in revised form 21 January 2004

## Abstract

Contour interpolation mechanisms allow perception of bounded objects despite incomplete edge information. Here, we introduce a paradigm that maps interpolated contours as they unfold over time. Observers localize dots relative to perceived boundaries of illusory, partly occluded, or control stimuli. Variations in performance with dot position and processing time reveal the location and precision of emerging contour representations. Illusory and occluded contours yielded more proficient dot localization than control stimuli containing only spatial cues, suggesting performance based on low-level representations. Further, illusory contours exhibited a distinct developmental time course, emerging over the first 120 ms of processing. These experiments establish the effectiveness of the dot localization paradigm for examining interpolated edge representations, contour microgenesis, and the underlying processing mechanisms.

© 2004 Elsevier Ltd. All rights reserved.

*Keywords:* Illusory contours; Interpolation; Filling-in; Occlusion; Localization

## 1. Introduction

Contour interpolation is a ubiquitous phenomenon. Every day, we confront numerous objects bounded by edges that are not fully defined by visual information. In many cases, the lack of visual specification stems from partial occlusion by surrounding objects; in other cases, incomplete edge specification arises from a lack of contrast with the background environment. Regardless, we often perceive the shapes of incompletely defined objects with ease, because contour interpolation processes “complete” the objects’ missing edges.

In situations of partial occlusion, contour interpolation leads to the perception of a clearly defined object boundary behind the occluding surface (Fig. 1a). When a surface lacks contrast with its surround, contour interpolation leads to the perception of illusory contours—edges perceived in the absence of any luminance, color, texture, depth, or motion discontinuities (Fig. 1b). Though seemingly different phenomena, theoretical arguments and empirical results suggest that partly occluded and illusory contours arise from a common

boundary interpolation process (e.g., Kellman, Guttman, & Wickens, 2001; Kellman & Shipley, 1991; Kellman, Yin, & Shipley, 1998; Shipley & Kellman, 1992). However, despite the importance of this process for our perception of objects, we are just beginning to understand the neural mechanisms and computational algorithms by which the edges of objects become completed.

One way to advance our knowledge of contour interpolation is by investigating edge representations as they emerge. In this paper, we describe a new dot localization paradigm, an extension of a method originated by Pomerantz, Goldberg, Golder, and Tetewsky (1981), that reveals both the shape and strength of interpolated contour representations as they unfold over time.<sup>1</sup> In our experiments, observers view stimuli containing illusory contours (see Fig. 1b). At some point during processing, a small dot is presented near one of the undefined contours, after which the entire stimulus configuration is masked. The observer makes a forced-choice judgment of whether the dot appeared inside or outside the perceived boundary of the illusory shape. Dot position varies through the method of constant stimuli or according to two interleaved staircase procedures

\* Corresponding author. Address: Department of Psychology, Vanderbilt University, 111 21st Ave. South, Nashville, TN 37203, USA. Tel.: +1-615-322-8768; fax: +1-615-343-8449.

E-mail address: [sharon.guttman@vanderbilt.edu](mailto:sharon.guttman@vanderbilt.edu) (S.E. Guttman).

<sup>1</sup> Preliminary results with a static variant of this method have been reported earlier (Kellman, Shipley, & Kim, 1996; Kellman, Temesvary, Palmer, & Shipley, 2000).

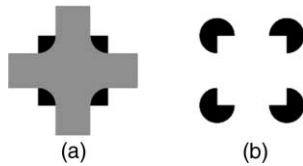


Fig. 1. Two examples of contour interpolation: (a) a partly occluded square; (b) an illusory square. The contours of both shapes may arise from a single boundary interpolation process.

that converge on different points of the underlying psychometric function. From these data, we estimate the *location* at which the observer perceives the interpolated contour and the *precision* of its representation. Further, by varying the duration of stimulus presentation, we map the emergence of interpolated contour representations over the course of visual processing.

Previous research suggests that boundary interpolation mechanisms produce spatially precise representations of illusory contours (e.g., Dresch & Bonnet, 1991, 1993; Greene & Brown, 1997; McCourt & Paulson, 1994). Moreover, a number of experiments indicate that observers can use interpolated contours to judge accurately the shapes of objects bounded by those contours (Gold, Murray, Bennett, & Sekuler, 2000; Pillow & Rubin, 2002; Ringach & Shapley, 1996). Therefore, if task performance reflects the presence of interpolated contours, then relatively accurate and precise dot localization should result. Alternatively, task performance could be based on recognition from partial information (Kellman et al., 2001) or other cognitive strategies that use visible edges as spatial cues, but without any contour interpolation. These cognitive strategies may ultimately result in “completed” shapes that appear quite similar to those resulting from interpolation processes. However, the edge representations emerging from cognitive strategies may be less spatially precise and less rapidly computed than edges interpolated through low-level mechanisms. Accordingly, one might expect “cognitive” edges to yield imprecise dot localization and to show temporal characteristics distinguishable from true cases of contour interpolation.

The prediction of precise contour interpolation—and the resulting precision of dot localization—applies specifically to the *final* outputs of the underlying processes. Despite the phenomenological experience of completion as instantaneous and effortless, research indicates that visual interpolation takes measurable time (e.g., Gegenfurtner, Brown, & Rieger, 1997; Guttman, Sekuler, & Kellman, 2003; Murray, Sekuler, & Bennett, 2001; Rauschenberger & Yantis, 2001; Ringach & Shapley, 1996; Shore & Enns, 1997). Thus, we expect to see improvements in dot localization performance as processing time increases. The form and time course of this improvement provide two important windows into the nature of contour interpolation processes.

The paradigm presented here resembles but extends procedures described previously (Pomerantz et al., 1981; Schoumans & Sittig, 2000; Takeichi, 1995). As in these other methods, observers judge the position of a dot relative to an interpolated object boundary. However, our approach differs in two respects. First, in addition to measuring the perceived *location* of illusory or partly occluded contours, which can be accomplished by measuring variations in reaction time (Pomerantz et al., 1981) or using a single 1-up/1-down staircase (Takeichi, 1995), our procedure extracts two different points on the underlying psychometric function to yield an objective measure of interpolated contour *precision*. Second, earlier methods typically presented stimuli until response (e.g., Pomerantz et al., 1981; Schoumans & Sittig, 2000); in our procedure, observers view the stimuli for a limited, measurable duration. In avoiding long image presentation, this new paradigm has a number of advantages. First, short-duration stimulus presentations reduce the probability that observers engage in cognitive processing strategies. Second, dots shown in combination with illusory stimuli may actually influence the shapes of interpolated contours (Gregory, 1972; Kanizsa, 1976; Schoumans & Sittig, 2000); however, this effect has been observed only with prolonged stimulus presentations. Third, and most important, by limiting stimulus presentation and probing contour representations at specific processing durations, one can map the microgenesis (developmental time course) of interpolated contour formation.

The first two experiments of the current study focused on testing whether the new dot localization paradigm reveals interpolated contour representations. In a third experiment, we examined the microgenesis of illusory contour representations during the first 320 ms of visual processing. The results of our investigations indicate the usefulness of the dot localization technique both for probing the final representations of interpolated contours and for investigating their visual evolution.

## 2. Experiment 1: Static representations of illusory contours

The first experiment tested dot localization performance for various stimuli, each processed for 200 ms. Specifically, we compared effects produced by images containing illusory edges with those produced by images containing luminance-defined edges, as well as stimuli containing comparable spatial cues—useful for cognitive judgments—but no relevant contour information.

When triggered by visible edges in appropriate spatial relationships, boundary interpolation mechanisms should, in theory, generate illusory contours in precise locations (e.g., Dresch & Bonnet, 1991, 1993; McCourt & Paulson, 1994). Therefore, if task performance with the

illusory stimuli reflects the operation of contour interpolation mechanisms, then the precision of dot localization may approach levels obtained with luminance contours and should exceed levels obtained with control stimuli containing only spatial cues. By contrast, if dot localization performance depends on spatial cueing without contour interpolation, or on other cognitive strategies, then precision levels obtained with the illusory and control stimuli should be similar.

## 2.1. Method

### 2.1.1. Observers

Forty-two UCLA undergraduate students (11 men and 31 women), ranging in age from 18 to 23 years (mean age = 20.2 years), participated in the experiment. The observers had normal or corrected-to-normal vision and were naive regarding the experimental hypotheses. All observers received partial course credit in an introductory psychology class in exchange for their participation.

### 2.1.2. Apparatus

The experimental trials were generated using a program written in MacProbe 1.8 (Hunt, 1994) on a PowerMac G4 with a 733 MHz processor. Observers viewed stimuli on a Viewsonic P224f 22" Color Monitor (75 Hz; 1280×1024 pixels) and responded by pressing one of two keys on the keyboard. Observers sat 57.3 cm from the screen with their heads stabilized in a chin-and-forehead rest.

### 2.1.3. Design

The experimental design included three crossed within-subject variables: *contour type* (illusory, real, or control), *stimulus shape* (square, fat, or thin), and *staircase direction* (inside or outside); thus, each observer completed 18 interleaved staircases, with trials from each staircase presented in random order. The nature of the *control stimulus* (arrow or rounded-TD) varied between observers.

### 2.1.4. Stimuli

Fig. 2 depicts the stimuli used in this experiment. The illusory contour stimuli (Fig. 2a) contained four black circles, each 2.0° in diameter and missing a 90° notch measuring 1.0° along each edge. The four notches faced inward to create an illusory shape. For the squares, the edges of the notches were horizontal and vertical; inducer rotations of  $\pm 15^\circ$ , with alternating inducers rotated in opposite directions, created fat and thin configurations (Ringach & Shapley, 1996). The center-to-center distance between the inducing elements measured 4.0°, thus yielding illusory shapes with a support ratio of 0.5.

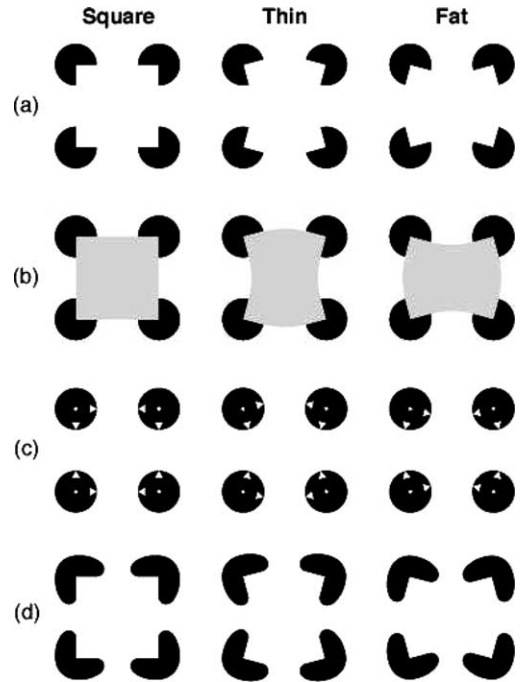


Fig. 2. Stimuli for Experiment 1: (a) illusory edges; (b) real edges; (c) arrow control; (d) rounded-TD control. The dot localization experiment used square, thin, and fat variants of each stimulus type.

The black elements of the real-contour stimuli (Fig. 2b) precisely matched those of the illusory stimuli. Additionally, a gray square, thin, or fat shape—fully defined by luminance edges—appeared in the center of the configuration. The curved edges of the fat and thin shapes followed an arc of constant curvature, tangential to the black inducing edges at the points of tangent discontinuity.

The “arrow” control stimuli (Fig. 2c) contained a small white circle (0.2° in diameter) in the center of each circular inducer and two triangular “arrows” (0.38° along each side). The points of the triangles met the edges of the inducing circle and mirrored the locations of the inducing contours in the shapes’ illusory counterparts.

The other set of control stimuli (Fig. 2d) contained salient inducing edges that precisely matched those of the illusory contour stimuli, but with curved corners rather than sharp tangent discontinuities (TDs); previous empirical studies have demonstrated that eliminating TDs from illusory contour displays dramatically reduces or eliminates the subjective experience of illusory contours (Rubin, 2001; Shipley & Kellman, 1990; Tse & Albert, 1998).<sup>2</sup> The “rounded-TD” stimuli originated from the same notched-circle inducers as their illusory counterparts. Beyond the straight inducing

<sup>2</sup> The occasional percept of weak interpolated contours in rounded-TD displays may be attributed to the registration of TDs in channels selective for low spatial frequency information (Kellman et al., 2001).

contours, the edges of the inducer curved outward along a circular arc ( $0.375^\circ$  in diameter). Additional black pixels ensured that the entire inducer had smooth edges. As with the other stimuli, four rounded-TD inducers were arranged such that the notches bounded a  $4.0^\circ$  square. Inducer rotations of  $\pm 15^\circ$  created the fat and thin configurations.

The black inducing elements measured  $4.2 \text{ cd/m}^2$  and appeared on a white background of  $121 \text{ cd/m}^2$ . The gray level of the luminance-defined shapes measured  $97.6 \text{ cd/m}^2$ , creating a Michelson contrast level of 10.7%.

Masking stimuli consisted of randomly sized ellipses of various gray levels, arranged so as to completely cover the stimulus region (see Fig. 3c). The gray levels of the ellipses in these masks covered the full range of luminance levels between the black and white values given above.

### 2.1.5. Procedure

A schematic illustration of the trial structure appears in Fig. 3. Each trial began with the presentation of four complete circles for 1000 ms (Fig. 3a); the position of these circles was jittered from trial to trial by up to  $1.0^\circ$  from the center of the screen. Next, a shape defined by illusory contours, luminance contours, arrows, or rounded-TD elements appeared for 200 ms, aligned with the complete circles in the previous frame (Fig. 3b); a small red dot ( $3.5 \text{ arcmin} \times 3.5 \text{ arcmin}$ ;  $25.7 \text{ cd/m}^2$ ) was superimposed on the stimulus near the top contour (or equivalent) of the stimulus shape. Finally, a mask appeared until response (Fig. 3c).

Observers judged whether the red dot appeared inside or outside the perceived boundary of the illusory or real shape. For control stimuli, instructions indicated that observers should imagine a shape with edges that smoothly joined the visible cues as in the corresponding real shapes, and should judge dot position relative to the imagined shape. Observers reported their percepts by pressing one of two keys; no feedback was given. Each trial was initiated by a spacebar press, producing a variable intertrial interval.

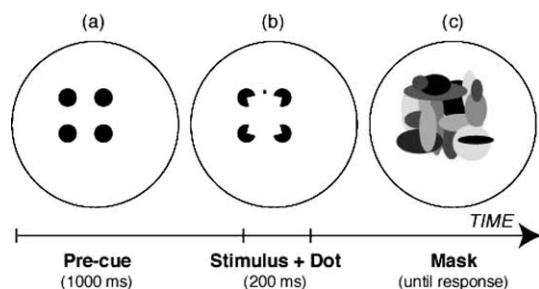


Fig. 3. Trial structure for Experiment 1: (a) pre-cue; (b) stimulus with superimposed dot; (c) mask. The dot is not drawn to scale; in the experiment, the dot was significantly smaller, relative to the stimulus.

For each stimulus, the position of the probe dot varied based on two interleaved staircases. The *inside* (3-up/1-down) staircase converged on the point of the underlying psychometric function at which the observer was 0.79 likely to respond that the dot appeared “inside” the shape’s boundary; the *outside* (3-down/1-up) staircase converged on the point of the psychometric functions at which the observer was 0.79 likely to respond that the dot appeared “outside” the shape’s boundary (Derman, 1957). For the inside staircases, the probe dot initially appeared midway between the upper two inducing stimulus elements,  $17.6 \text{ arcmin}$  below the theoretical contour position. The dot remained in this position until the observer made three consecutive “inside” responses or a single “outside” response to the stimulus in question. Three “inside” responses caused the dot to appear at a higher position on the next trial with that staircase (i.e., less inside the object’s boundary), thus making the task more difficult. By contrast, a single “outside” response caused the dot to appear at a lower position on the next trial (i.e., *more* inside the object’s boundary), thus making the task easier. For the outside staircases, this procedure was reversed: The probe dot initially appeared midway between the upper two inducing elements, but  $17.6 \text{ arcmin}$  above the theoretical contour position. Three consecutive “outside” responses caused the dot to appear in a lower position on the next trial (i.e., less outside), whereas a single “inside” response caused the dot to appear in a higher position on the next trial (i.e., more outside).

The probe dot always appeared along an imaginary vertical line, half way between the upper two inducing elements. Changes in dot position occurred in  $8.8 \text{ arcmin}$  increments until the staircase underwent two reversals of direction in the dot’s position changes. Next, the dot shifted position in  $5.3 \text{ arcmin}$  increments for four reversals. Completion of the staircase required 11 reversals with the dot shifting position in  $1.8 \text{ arcmin}$  increments (Falmagne, 1986). The experiment continued until all staircases converged, which typically required approximately 50 min. Observers received a short break every 200 trials.

### 2.1.6. Analysis

For each staircase, the dot locations giving rise to the final 10 reversals were averaged. This averaging revealed the points on the underlying psychometric function at which the observer was 0.21 and 0.79 likely to report that the dot appeared outside of the stimulus shape’s perceived boundary; these points are deemed the *inside threshold* and *outside threshold*, respectively (Fig. 4). Both thresholds contributed to three dependent measures.

The *location* measure produced an estimate of where the observer perceived the object boundary. We defined location as the midpoint between the inside and outside

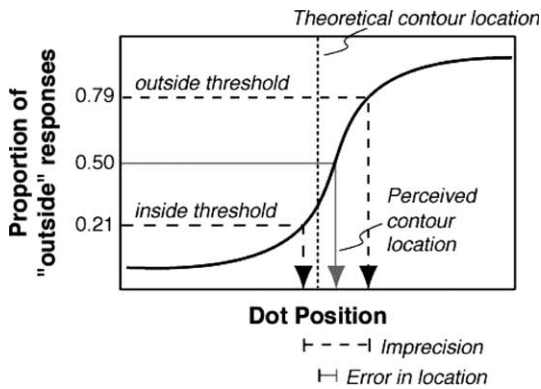


Fig. 4. Schematic illustration of the psychometric function underlying dot localization responses, and the dependent variables related to this function. See text for details.

thresholds, relative to the theoretical (or actual) boundary, assuming completion with a constant-curvature contour (Kellman & Shipley, 1991). This midpoint should be equal to the observer’s 0.50 probability of making an “outside” response if the psychometric function is rotationally symmetric about the 0.50 point. For this measure, a negative value indicated that the observer perceived the object boundary to be inside of its theoretical location, whereas a positive value indicated that the observer perceived the object boundary to be outside of its theoretical location. A location value of zero suggested that the observer perceived the boundary to be in its exact theoretical location. The *error in location* measure, calculated as the absolute value of location, indicated the accuracy of performance—how far from its theoretical location the contour was perceived, regardless of direction. Finally, the *imprecision* measure was defined as the distance between the inside and outside thresholds for a given stimulus (see Fig. 4). The greater this distance, the less precisely the dot could be localized, relative to the stimulus boundary. These latter two measures should be highly correlated, as stronger contour representations should yield both greater precision within observers and lower variability between observers (and thus higher accuracy, assuming a reasonable theoretical model of contour shape).

The data from one observer were discarded due to an inability to perform the task. (Imprecision levels for all stimuli, including those with real contours, lagged the levels of other observers by an order of magnitude.) A second observer’s data were discarded because two staircases failed to converge within a one hour session. The location, error in location, and imprecision data from the 40 remaining observers entered  $3 \times 3 \times 2$  ANOVAs with contour type and stimulus shape as within-subject variables and control stimulus as a between-subjects variable. Additionally, planned *t*-tests compared the error and imprecision results obtained with each illusory stimulus to the results obtained with

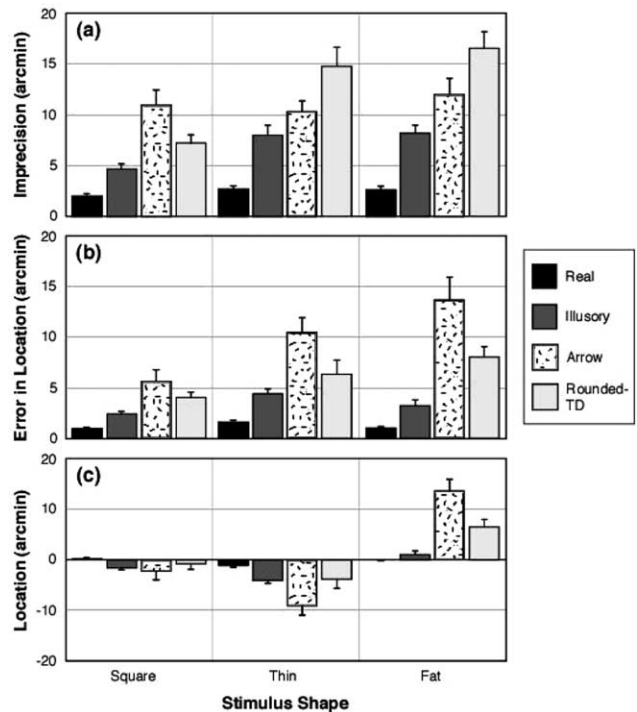


Fig. 5. Results of Experiment 1, plotted by stimulus shape and contour type: (a) imprecision; (b) error in location; (c) location data, where positive values indicate perception of the contour as outside of its theoretical position and negative values indicate perception of the contour as inside of its theoretical position. For all graphs, error bars represent  $\pm 1$  standard error across observers.

its real-contour, arrow, and rounded-TD counterparts. Other planned *t*-tests compared results with the three illusory shapes to one another, collapsed across the two groups of observers. Planned comparisons on the location data determined which of the illusory stimuli became completed along paths that differed significantly from the constant-curvature model (i.e., which values deviated from zero).

## 2.2. Results

Fig. 5 depicts the experimental results by contour type and stimulus shape. Higher values on these graphs indicate less proficient task performance. For all graphs, plotted values for the illusory and real-contour stimuli indicate the average across the two groups of observers.<sup>3</sup>

<sup>3</sup> Statistical testing—ANOVAs conducted with only the illusory and real contour stimuli—indicated that the control condition had no effect on results with these stimuli, which were identical for all observers ( $F < 1$  for main effect and all relevant interactions on all three measures).

The imprecision and error in location results (Fig. 5a, b, respectively) most directly address the dot localization paradigm's sensitivity to contour representations. Overall, stimuli with luminance-defined contours produced the most precise dot localization, followed by the stimuli with illusory contours; the arrow and rounded-TD control stimuli, which contained comparable spatial cues but no clear interpolated contours, led to the least precise task performance {overall  $F(2, 76) = 98.2$ ,  $p < 0.001$ }. Similarly, illusory contours produced more accurate task performance (i.e., smaller errors in location) than the arrow and rounded-TD control stimuli, but less accurate performance (i.e., larger errors in location) than the real contour stimuli {overall  $F(2, 76) = 102.3$ ,  $p < 0.001$ }. The planned  $t$ -tests generally supported these findings; with one exception, the illusory contour stimuli differed significantly from both their real-contour and control counterparts on both the imprecision and error in location measures  $\{t_{19} = 1.58$ ,  $p = 0.13$  for the comparison between the thin illusory and thin rounded-TD shapes on error in location;  $p < 0.05$  for all other pairwise comparisons}.

This pattern of results is consistent with the notion that observers judge dot location relative to a contour representation, if available, thus producing more precise and accurate task performance than can be achieved through cognitive strategies. By this explanation, the observed differences in dot localization between the real contour and illusory contour stimuli reflect the relative strengths of luminance-defined versus interpolated contour representations. The inferior performance with the control stimuli may be attributed to cognitive strategies relying on spatial cues, as the arrow and rounded-TD stimuli do not lead to well-specified contour representations.

The imprecision and error in location data also suggest that straight contours may be more strongly interpolated than curved contours (see Fig. 5a, b). Across all contour types, stimulus shape significantly affected dot localization precision  $\{F(2, 76) = 42.7$ ,  $p < 0.001$ } and accuracy  $\{F(2, 76) = 7.8$ ,  $p < 0.01$ }. Additionally, contour type and stimulus shape produced significant interactions on both dependent measures  $\{F(4, 152) = 8.4$ ,  $p < 0.001$  for imprecision;  $F(4, 152) = 10.7$ ,  $p < 0.001$  for error in location}. Most telling, although the pairwise comparisons revealed that the fat and thin illusory contour shapes resulted in similar levels of dot localization performance  $\{t_{39} < 1.5$  for both imprecision and error in location}, observers generally localized the edges of the illusory squares more precisely and accurately than the edges of the curved (fat or thin) shapes  $\{t_{39} = 1.51$ ,  $p = 0.14$  for the comparison of square and fat shapes on error in location;  $p < 0.001$  for all other comparisons}. This decrease in illusory contour strength with increasing curvature has been observed with other perceptual tasks (e.g., Shipley & Kellman, 1992). Thus,

the current effect of shape supports the notion that the dot localization paradigm probes interpolated contour representations.

The overall analyses of precision and accuracy also revealed some interesting differences between the two groups of observers, who viewed different control stimuli. On the error in location measure, the control stimulus led to a significant main effect  $\{F(1, 38) = 6.9$ ,  $p < 0.05$ } and interacted with contour type  $\{F(2, 76) = 8.2$ ,  $p < 0.01$ }; no other interactions approached significance. An examination of Fig. 5b (as well as an analysis confirming that results with the illusory and real-contour stimuli did not differ across the two groups) reveals that these effects can be attributed to larger errors in location with the arrow stimuli than with the rounded-TD stimuli.

Somewhat different effects of control stimulus arose on the imprecision measure: Neither a main effect nor a simple interaction with contour type were observed. Rather, control stimulus interacted significantly with stimulus shape  $\{F(2, 76) = 10.7$ ,  $p < 0.001$ } and was involved in a 3-way interaction with stimulus shape and contour type  $\{F(4, 152) = 10.7$ ,  $p < 0.001$ }. Whereas precision with the arrow stimuli did not depend on stimulus shape, the pattern of precision results across shapes in the rounded-TD stimuli mirrored the pattern with the illusory stimuli. Post hoc analyses ( $t$ -tests conducted with  $\alpha = 0.05$ , Bonferroni correction) indicated that rounded-TD squares led to more precise dot localization than the corresponding thin and fat shapes  $\{t_{19} = 4.9$ ,  $p < 0.001$ ;  $t_{19} = 6.5$ ,  $p < 0.001$ }, but the two curved shapes did not differ significantly from one another  $\{t_{19} = 2.1$ ,  $p = 0.052$ }. This pattern was *not* observed with the arrow stimuli, on which all three shapes led to similar precision levels. The effect of curvature in the rounded-TD stimuli suggests that the visual system may have interpolated "fuzzy" contours between the rounded-TD inducers, due to low spatial frequency information consistent with the conditions necessary for interpolation. The greater accuracy with these stimuli than with the arrow stimuli coheres with this interpretation.

The location measure addresses the form of interpolated contours. For the location graph (Fig. 5c), positive values indicate perception of the contours as outside of their theoretical positions, whereas negative values indicate perception of the contours as inside of their theoretical positions. Both stimulus shape and contour type had significant effects on perceived contour location  $\{F(2, 38) = 82.3$ ,  $p < 0.001$ ;  $F(2, 38) = 5.32$ ,  $p < 0.01$ , respectively}. The interaction between these factors also reached significance  $\{F(4, 76) = 82.5$ ,  $p < 0.001$ }. Additionally, the larger errors in location with the arrow stimuli than with the rounded-TD stimuli, particularly with the curved shapes, were reflected in these data by a significant interaction between control stimulus and

contour shape  $\{F(2, 76) = 9.1, p < 0.001\}$  and a 3-way interaction  $\{F(4, 152) = 13.6, p < 0.001\}$ .

In the current context, however, the perceived location of the illusory contours warrants the most attention. The illusory contours of the squares, despite little apparent ambiguity in their shape, tended to be perceived as slightly inside of their theoretical position  $\{t_{39} = -4.4, p < 0.001\}$ . This effect may reflect a modest “shrinkage” of the illusory shape, or, alternatively, a slight bias to respond “outside” under conditions of perceptual uncertainty. The perceived location data further indicate that the illusory contours of the thin shapes tended to be reported in locations somewhat inside of their theoretical position  $\{t_{39} = -7.3, p < 0.001\}$ , whereas the illusory contours of the fat shapes tended to be reported in locations slightly, though not significantly, outside of their theoretical position  $\{t_{39} = 1.3, p = 0.19\}$ . These findings are consistent with the idea that observers interpolated slightly “flatter” contours than predicted by constant-curvature arcs tangential to the inducing edges at the points of discontinuity. If adjusted for the bias suggested by the data with the illusory squares, then the thin and fat illusory contours appear to have been completed along similarly curved paths.

### 2.3. Discussion

Experiment 1 sought to validate the dot localization paradigm by comparing performance between stimuli that contain edge representations and those that do not. Not surprisingly, stimuli with luminance edges yielded the most proficient task performance. However, illusory contour stimuli produced more precise and more accurate performance than the arrow or rounded-TD controls, both of which contain salient spatial cues but no clear interpolated contours. As results with the control stimuli provide indices for precision and accuracy levels achievable through cognitive inference alone, the superior performance with the illusory stimuli suggests the operation of lower-level contour interpolation mechanisms. Furthermore, stimuli that induce curved interpolated edges generally produced less precise and accurate dot localization than stimuli that permit linear interpolation; this finding corresponds both to studies of contour interpolation using different methods (e.g., Shipley & Kellman, 1992) and to studies of the integration of real contour segments (e.g., Field, Hayes, & Hess, 1993). Thus, the dot localization task appears to probe the visual representations of both real and interpolated contours.

Although not the primary focus, Experiment 1 also indicated that the dot localization task might be fruitful for determining the shapes of interpolated contours. Task performance with the illusory contour stimuli suggested that edges may be interpolated along curvi-

linear paths that are “flatter” (i.e., contain less curvature) than predicted by a constant-curvature model. The observed deviations from the predicted contour locations were quite small, both relative to measured precision and in absolute terms (e.g., a 3 arcmin deviation equals 0.5 mm at the viewing distance used here). Even so, the consistency of these effects is interesting, and suggests that dot localization may be used to explore how the exact forms of interpolated contours compare to the predictions of various models (e.g., Fantoni & Gerbino, 2003; Kellman & Shipley, 1991; Ullman, 1976). However, caution may be required in this regard; the control stimuli showed little evidence of contour interpolation, yet exhibited even stronger tendencies to minimize curvature than the illusory contour stimuli. This observation suggests that, under conditions of perceptual uncertainty, observers’ responses may regress toward the average contour position. Nevertheless, with further efforts to disentangle response bias from the effects of perceptual representations, the dot localization paradigm may be an effective tool for determining the shapes of interpolated boundaries.

### 3. Experiment 2: The identity hypothesis

Several perceptual phenomena, in addition to illusory contour formation, involve the operation of boundary interpolation mechanisms. The completion of partly occluded contours is one such phenomenon. Thus, if dot localization performance reflects interpolated contour representations, then the paradigm should be sensitive to edges completed behind an occluder, just as it is to illusory edges. Experiment 2 tests the generality of the dot localization paradigm by comparing task performance between illusory and partly occluded stimuli, relative to control stimuli containing only spatial cues. As a general probe for interpolated contour representations, we expect to see more precise and accurate dot localization with both illusory and partly occluded stimuli than with their respective controls.

Experiment 2 also allowed comparison of illusory contour formation and occluded contour completion to one another. This comparison has relevance to the *identity hypothesis* in visual interpolation (Kellman & Shipley, 1991). The identity hypothesis, which is supported by both theoretical arguments (e.g., Kellman et al., 2001) and previous empirical findings (e.g., Kellman et al., 1998; Shipley & Kellman, 1992), proposes that the interpolation of illusory and partly occluded contours arises from a *common* mechanism. By this hypothesis, the illusory stimuli and their occluded counterparts should not only produce better task performance than that obtained with the spatial-cue control stimuli, but *comparable* dot localization precision and accuracy to one another. Further, the identity hypothesis predicts

that the contours of the illusory and partly occluded stimuli will follow the same interpolated path, and thus be localized in the same position.

3.1. Method

Twenty-two naive observers (7 men and 15 women), all with normal or corrected vision and ranging in age from 18 to 22 years (mean age = 19.4 years), participated in the experiment. The data from two observers were excluded from the final analysis because one or more of their staircases failed to converge within a 90 min session. Two additional observers misunderstood the task for the occluded stimuli, judging dot position relative to the occluder rather than the occluded shape, so these data were discarded as well. Therefore, the data from 18 observers entered the final analyses.

The experiment closely resembled Experiment 1, except that each observer judged dot location relative to four contour types: illusory, illusory-control, occluded, and occluded-control. The illusory and illusory-control stimuli were identical to the illusory and arrow stimuli used in Experiment 1 (see Fig. 2a, c, respectively). Fig. 6 depicts the occluded and occluded-control stimuli. These stimuli contained a white cross-shaped inducer bounded by a 1.8 arcmin gray contour (20.4 cd/m<sup>2</sup>). The white inducer ensured that the contrast between the dot and the background remained equal across the illusory and occluded stimuli. The occluder measured 6.0° along its greatest vertical and horizontal extents. The segment removed from each corner had the shape of a half circle, 2.0° in diameter, projected toward the associated corner with tangential extensions. The distance between two of the round notches at closest approach measured 2.0°.

The occluded stimuli (Fig. 6a) had four visible black corners; the inducing edge of each measured 1.0° in length and precisely matched the length and location of the inducing edges in the corresponding illusory shape. The occluded-control stimuli (Fig. 6b) had a black dot and two black triangles in each corner that precisely matched the white elements of the corresponding illu-

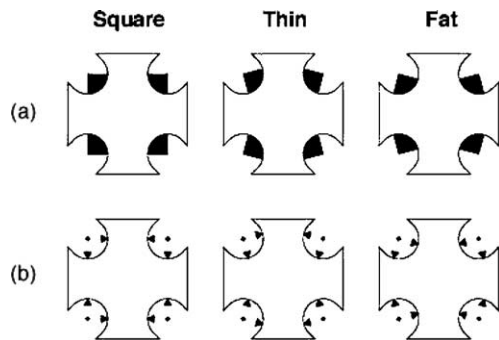


Fig. 6. New stimuli for Experiment 2: (a) occluded; (b) occluded-control. The dot localization experiment used square, thin, and fat variants of each stimulus type.

sory-control inducers. All other aspects of the stimuli, including the use of square, fat, and thin variants of each type, corresponded to Experiment 1.

The procedure mirrored that of Experiment 1; however, because each observer viewed all four contour types, Experiment 2 involved the convergence of 24 staircases per observer, rather than 18. The imprecision, error in location, and location data entered repeated-measures 4 × 3 ANOVAs with contour type and stimulus shape as the independent variables. Additionally, 2 × 3 ANOVAs with each dependent measure tested directly for differences between the illusory and occluded stimuli.

3.2. Results

If the dot localization paradigm probes interpolated contour representations, then both the illusory and occluded figures should yield dot localization precision and accuracy levels that exceed those of their arrow-control counterparts. Further, the identity hypothesis predicts that the two types of interpolated figures will produce comparable levels of precision and accuracy. The experimental results, depicted in Fig. 7, support these predictions.

As anticipated, stimulus type had significant effects on both dot localization precision { $F(3, 51) = 17.1$ ,

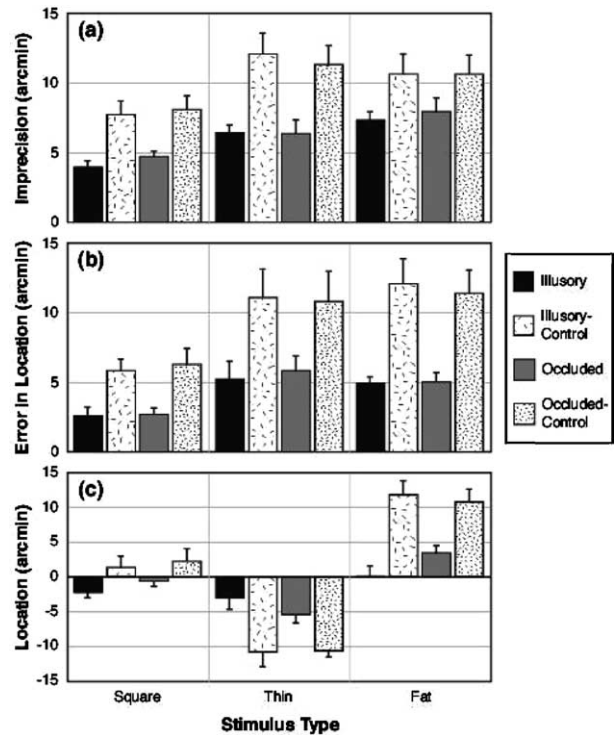


Fig. 7. Results of Experiment 2, plotted by stimulus shape and contour type: (a) imprecision; (b) error in location; (c) location data, where positive values indicate perception of the contour as outside of its theoretical position and negative values indicate perception of the contour as inside of its theoretical position. For all graphs, error bars represent ±1 standard error across observers.

$p < 0.001$ } and accuracy  $\{F(3, 51) = 34.5, p < 0.001\}$ . These effects can be attributed entirely to differences between the interpolated stimuli and the control stimuli. When compared directly, statistical analyses revealed no reliable differences between the illusory and occluded shapes on either the imprecision or error in location measures  $\{F(1, 17) < 1$  for both analyses}. These findings coincide with the identity hypothesis, and support the notion that the dot localization paradigm probes the spatially precise boundary representations arising from interpolation processes.

The results of Experiment 1 suggested that the visual system may interpolate straight contours more strongly than curved contours. Experiment 2 further supports this hypothesis. As before, stimulus shape significantly affected both the precision and accuracy of dot localization  $\{F(2, 34) = 10.2, p < 0.001; F(2, 34) = 4.32, p < 0.05, \text{ respectively}\}$ . The interaction between stimulus shape and contour type did not approach significance on either measure  $\{F(6, 102) \approx 1\}$ . Importantly, however, a clear effect of shape still emerged when considering the interpolated shapes in isolation  $\{F(2, 34) = 22.9, p < 0.001$  for imprecision;  $F(2, 34) = 5.12, p < 0.05$  for error in location}. Thus, it appears that observers can localize the contours of illusory and occluded squares more precisely and accurately than the contours of comparable illusory and occluded curved-edge shapes.

The location data, which appear in Fig. 7c, revealed the extent to which a constant-curvature completion can account for perceived stimulus shape. Predictably, observers perceived the contours of the illusory and occluded shapes as closer to their theoretical positions than they did with the control stimuli  $\{F(3, 51) = 3.23, p < 0.05\}$ . Additionally, the main effect of shape reached significance  $\{F(2, 34) = 88.4, p < 0.001\}$ . Observers localized the contours (or equivalent) of the squares quite close to the theoretical location. However, as in Experiment 1, observers tended to localize the edges of the thin shapes as inside of their theoretical location and the edges of the fat shapes as outside of their theoretical location. Because of the larger errors overall, the differences between shapes were more pronounced with the control stimuli than with the interpolated stimuli, resulting in a significant interaction  $\{F(6, 102) = 52.2, p < 0.001\}$ .

The direct comparison of illusory and occluded shapes confirmed that stimulus shape had a significant effect on perceived location of the interpolated contours  $\{F(2, 34) = 17.7, p < 0.001\}$ . This analysis also revealed small differences between the illusory and occluded contour completions. Although the main effect of contour type on perceived location did not reach significance  $\{F(1, 17) = 3.15, p = 0.09\}$ , a significant interaction between contour type and stimulus shape emerged  $\{F(2, 34) = 25.9, p < 0.001\}$ . Post hoc comparisons indicated that all three illusory shapes differed

significantly, though by small amounts (2–3 arcmin), from their occluded counterparts  $\{p < 0.05/3$  for all  $t$ -tests}. For the curvilinear interpolations, Fig. 7c suggests that observers produced flatter completions of the occluded shapes than the illusory shapes. This finding represents a small, though potentially interesting, deviation from the identity hypothesis (Kellman & Shipley, 1991; Shipley & Kellman, 1992).

### 3.3. Discussion

The results of this experiment support the notion that the dot localization paradigm probes interpolated contour representations and extend the method's use to partly occluded stimuli. Both illusory and partly occluded shapes yielded more precise and accurate task performance than the control stimuli containing comparable spatial cues but no interpolated contours. Moreover, the precision and accuracy levels obtained with occluded contours confirm other indications (e.g., Gold et al., 2000; Guttman et al., 2003) that the visual system represents occluded contours with considerable local precision. These findings are more consistent with views characterizing occluded contours as a product of spatially precise visual interpolation processes rather than as resulting from cognitive inferences or recognition from partial information.

The second motivation for Experiment 2 involved exploring the identity hypothesis (Kellman & Shipley, 1991; Shipley & Kellman, 1992) with a paradigm that may be more sensitive to subtle differences in contour representations than those previously employed. In general, the illusory and partly occluded shapes produced very similar levels of dot localization precision and accuracy, as would be expected if their contours arose from the same basic interpolation mechanism. However, the location data indicated that the curved occluded contours tended to be perceived as slightly flatter than the curved illusory contours. This previously unobserved difference may reflect an influence of global context—other contours and surfaces in the scene—on interpolated contour shape (Guttman et al., 2003). Similar influences of global context occur in some illusions of visual space (e.g., the Poggendorf and twisted cord illusions), whereby the presence of “irrelevant” contours causes slight alterations in the perceived orientation or position of other contours. Thus, although interpolation across gaps may begin with a common mechanism—as suggested by the correspondence between the illusory and partly occluded contours on the imprecision and error in location measures—the final representations of contours likely reflect both local edge relationships and more global stimulus interactions. Rather than envisioning multiple interpolation processes, we suggest that the subtle deviations observed in interpolated contour shape may be explained by these global influences.

#### 4. Experiment 3: The microgenesis of illusory contours

The experiments discussed thus far validated the dot localization paradigm for a single processing duration: 200 ms. Our final experiment extended the methodology into the temporal dimension. In this study, stimulus duration varied from trial to trial and the dot appeared only during the last 40 ms of stimulus presentation. Thus, boundary interpolation mechanisms—and other visual processes—operated for variable amounts of time before their representations were probed. In this manner, we examined the microgenesis of illusory contour representations, as well as the representations of stimuli containing real edges or arrow location cues. Thus, Experiment 3 explored the usefulness of the dot localization paradigm for investigating the time course of boundary interpolation and sought information regarding the nature and time course of underlying completion mechanisms.

##### 4.1. Method

###### 4.1.1. Observers

Three naive observers, aged 18, 20, and 24 years, participated in the experiment. The one man and two women all had normal or corrected-to-normal vision and minimal previous experience with psychophysical experimentation.

###### 4.1.2. Design

The experiment consisted of the factorial combinations of four factors: *contour type* (illusory, real, or arrow control), *stimulus shape* (thin or fat), *stimulus onset asynchrony* (SOA; 40–200 ms in 13.3 ms increments, 240 ms, or 320 ms), and *dot location* (18 values per stimulus, centered around the theoretical position of the stimulus' top contour). In each of 20 experimental sessions, observers viewed every combination of these factors once, in random order, for a total of 1620 trials per session.

###### 4.1.3. Stimuli

The stimuli resembled the thin and fat illusory, real-contour, and arrow-control shapes used in Experiment 1 (see Fig. 2), but expanded by 150% so that the inducers measured  $3.0^\circ$  in diameter and the illusory shapes (and their counterparts) measured  $6.0^\circ$  from corner to corner.<sup>4</sup> Additionally, this experiment utilized a modified

version of the arrow controls, in which “teardrops” replaced the equilateral triangles as indicators; this change eliminated any ambiguity in the pointer direction. Each teardrop measured  $0.75^\circ$  in length and  $0.86^\circ$  in width. All other stimulus parameters matched those of Experiment 1.

###### 4.1.4. Procedure

In order to ensure equal detectability of the dot at the various stimulus presentation durations, the trial structure deviated slightly from earlier experiments. Specifically, the stimulus appeared on the screen prior to the probe dot; the dot was superimposed on the stimulus only during the last 40 ms of stimulus presentation. The SOA, a manipulated factor, included the entire duration for which the stimulus appeared (both with and without the dot), prior to masking. All other aspects of the trial structure matched those of Experiment 1 (see Fig. 3).

As in the other experiments, observers judged whether the dot appeared inside or outside the perceived boundary of the stimulus. However, to ensure the distribution of any fatigue or practice effects across the different conditions, dot location varied according to the method of constant stimuli, rather than staircase procedures. In this manner, observers responded to one example of each trial type during every session, instead of focusing on a single SOA in a single session (as the staircase method would have necessitated). The dot locations all fell along an imaginary vertical line, half way between the top two inducing elements. The 18 locations used per stimulus, spaced at 3.5 arcmin increments, straddled the theoretical contour position for the shape in question (assuming a smooth, constant-curvature completion).

Before beginning the experimental sessions, each observer completed eight practice sessions in which they viewed the various stimuli for 40, 80, 120, or 200 ms, with dot position varying by a staircase procedure. The 20 subsequent experimental sessions each contained 1620 randomly ordered trials (3 contour types  $\times$  2 stimulus shapes  $\times$  15 SOAs  $\times$  18 dot locations). Each session lasted approximately 1 h. Observers received a short, self-paced break every 180 trials.

###### 4.1.5. Analysis

The constant stimuli methodology necessitated a new procedure for calculating location and precision. For each observer, the data from the 20 sessions were combined and considered as a whole. The first step of the data analysis involved extracting basic psychometric functions for each combination of contour type, stimulus shape, and SOA. The resulting psychometric curves indicated the proportion of trials on which the observer responded “outside” as a function of dot position.

<sup>4</sup> Pilot testing with the larger stimuli produced a pattern of results resembling that of Experiment 1, but with the imprecision and error in location data scaled in proportion to stimulus size. The larger size was used here to ensure maximal detectability of any differences across the various stimuli.

Second, each of these data sets was fit with a three-parameter logistic function, described by the following equation:

$$y = \delta + \frac{1 - 2\delta}{1 + e^{\alpha(\mu - x)}} \quad (1)$$

where  $\alpha$  described the slope of the curve,  $\mu$  defined the midpoint around which the curve is rotationally symmetric, and  $\delta$  determined the minimum and maximum values of the function. In theory, these psychometric curves should range from 0 to 1; however, a certain number of erroneous button presses occurred over the course of 20 sessions, thus reducing the measured ranges of the functions. The  $\delta$ -value, estimated from the best fit to each data set, reflected the random error, allowing for more accurate estimates of slope. However, as  $\delta$  accounted for random error, values theoretically should be greater than or equal to zero, and equal across all conditions for a given observer. Therefore, for each observer, the mean  $\delta$  across all trial types was calculated, with any negative estimates being set to 0. The data sets then were refit using a two-parameter logistic function ( $\alpha, \mu$ ) with  $\delta$  set to the calculated constant.

Perceived location and imprecision of the interpolated boundary (or equivalent) depended on the  $\alpha$  and  $\mu$  leading to the best fit of the data (least squares method). The  $\mu$  values reflected perceived location. Imprecision equaled the distance between the dot locations giving rise to the 0.25 and 0.75 points on the psychometric function, assuming that the curves actually ranged from 0 to 1 (Eq. (2)).

$$\text{imprecision} = \frac{\log_e\left(\frac{1}{0.25} - 1\right) - \log_e\left(\frac{1}{0.75} - 1\right)}{\alpha} \quad (2)$$

Next, imprecision and perceived location data were plotted as functions of SOA. Information about asymptotic dot localization performance was extracted by fitting various functions of SOA with two-segment splines, each consisting of a quadratic segment followed by a flat line; these two segments met tangentially at one of the SOAs tested in the experiment. The three parameters of the spline model— $\tilde{x}_2$ ,  $a$ , and  $\tau$ —represented the image duration of the inflection point, the slope of the quadratic, and the constant of the flat line, respectively, calculated so as to minimize the energy of the model. The mathematical details of the spline formulation appear in Appendix A.

All curve fits omitted the two longest SOAs—240 and 320 ms. Observers' data sometimes showed a slight increase in imprecision and error in location at these durations, which introduced an obstacle to the curve fitting. However, there are several reasons to believe that

the increases, when they occur, do not reflect a meaningful deficit in performance.<sup>5</sup>

Based on their theoretical and previous empirical similarity, as well as a visual inspection revealing no consistent differences, data from the corresponding fat and thin shapes were combined to yield a single estimate of imprecision. Spline fits of the individual data revealed the asymptotic levels of performance for each observer. Spline fits of the imprecision data, averaged across observers, further revealed the SOA at which precision with the different contour types typically reached asymptote.<sup>6</sup>

For the location data, spline fits of individual data revealed the points at which observers ultimately perceived the contours of the illusory, real, or control stimuli; for this examination, fat and thin shapes were examined separately. Finally, splines were fit to the error in location data for each stimulus type, combined across shapes and observers, to achieve estimates of average accuracy level and time to asymptote.

#### 4.2. Results

Fig. 8 depicts each observer's imprecision results for the different contour types as functions of image duration. An examination of these graphs revealed two obvious effects. First, illusory contours produced more precise dot localization performance than the arrow control stimuli, but less precise performance than real edges, at all tested SOAs. Asymptotic imprecision values, obtained through the curve-fitting procedures described above and presented on the right side of each plot, confirmed that—for all observers—real edges produced the most precise dot localization performance, followed by illusory contours. The arrow controls, which contained comparable spatial cues but no edges capable of supporting interpolation, produced the least precise performance.

<sup>5</sup> The decline likely resulted from discontinuity in the step size between successive image durations at 240 and 320 ms. Because of the sudden jump after 200 ms, observers may have found that these longer durations contradicted expectations, thus diminishing performance. Further, given the large differences between these durations and the others, which were tested in 13.3 ms increments, practice effects may have generalized among the many shorter durations more than with the longer durations. Of note, similar increases were observed in several pilot experiments, regardless of the values of the last two durations. This finding indicates that the diminishing performance at the longest presentation durations reflects some aspect of the task, rather than a processing deficit that suddenly arises at 240 ms.

<sup>6</sup> Because of noise in individual observers' data, several different values of  $\tilde{x}_2$  often led to comparable fits, particularly with the location data. When this occurred, the choice of inflection points had little impact on estimates of  $\tau$ , the asymptotic performance levels. However, stable estimates of time-to-asymptote could consistently be achieved only on the group averages.

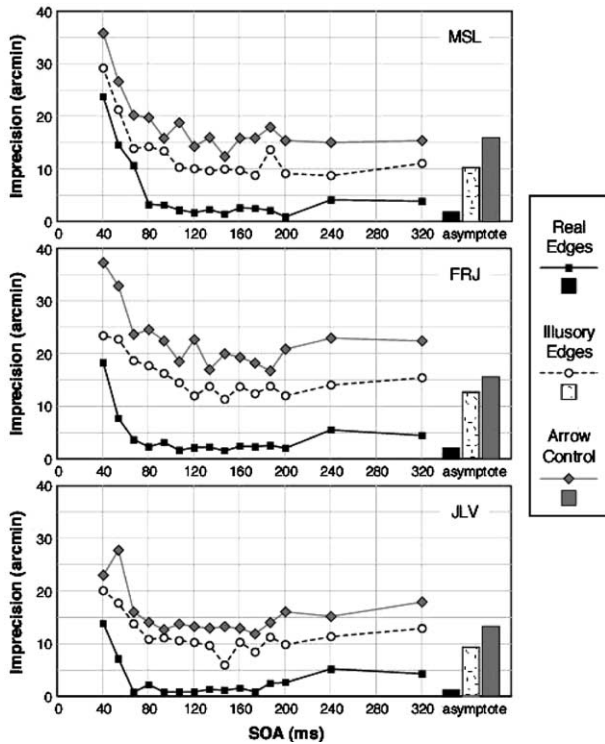


Fig. 8. Individual observers' imprecision results for Experiment 3. Imprecision appears as functions of SOA for the various contour types, averaged across fat and thin stimuli. Bars on the right side of each plot indicate asymptotic imprecision levels. Lower values on these plots indicate superior performance.

Second, imprecision of illusory contour perception decreased monotonically and rapidly with exposure duration. There did not appear to be any initial period in which precision remained steady. The fits of the group data revealed that, on average, precision of the illusory contour representations reached asymptote at 120 ms (Fig. 9). By contrast, perception of the real contours reached maximal precision at 80 ms. The best fit of the control stimuli suggests that observers reached asymptotic performance at 106.7 ms; however, even at asymptote, precision with these stimuli remained poor.

Fig. 10 depicts the perceived locations of the contours for the various stimulus types. The data show greater variability across observers than the precision results. Nonetheless, some generalizations can be made. First, real contours produced the most accurate dot localization performance, followed closely by illusory contours. Although the arrow controls sometimes were localized accurately, they typically produced the largest deviations from the theoretical contour locations. The asymptotic perceived contour locations, depicted on the right side of each panel, also illustrate these trends.

The differences between the thin and fat stimuli cause more difficulty for drawing generalizations. Across observers, no consistent differences emerged in the perceived locations of fat and thin illusory contours. A

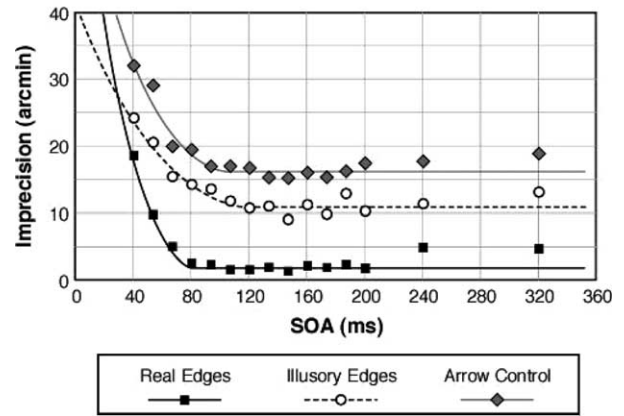


Fig. 9. Results of Experiment 3: Imprecision as a function of SOA, averaged across observers. The lines represent the best fitting splines, calculated with the last two data points of each set omitted. Imprecision of real edge perception reached an asymptote of 2.1 arcmin at 80 ms of image processing. Imprecision of illusory contour representations reached an asymptote of 10.9 arcmin after 120 ms of processing. Imprecision of performance with the arrow controls reached an asymptote of 16.1 arcmin after 106.7 ms of processing.

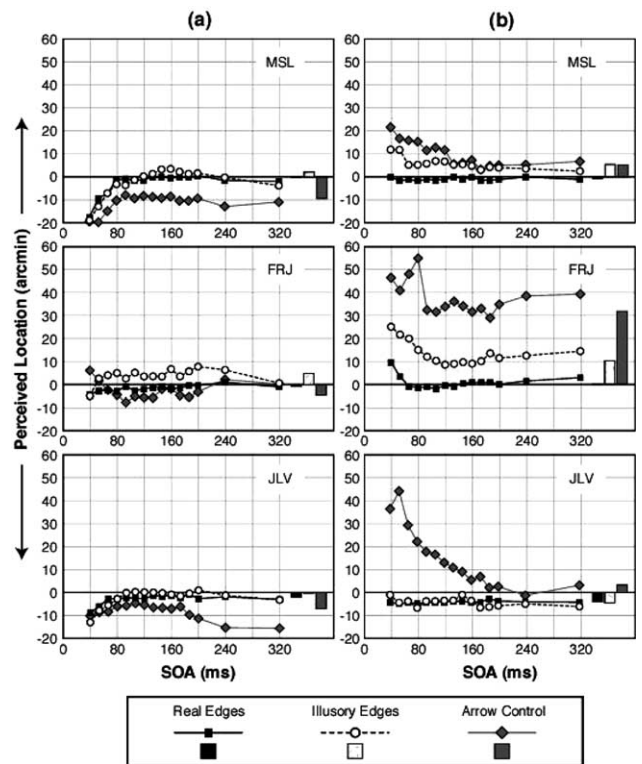


Fig. 10. Individual observers' perceived location results for Experiment 3, plotted as functions of SOA: (a) thin shapes; (b) fat shapes. Bars on the right side of each plot indicate asymptotic performance levels. Positive values reflect perception of the contours as outside of their theoretical locations; negative values reflect perception of the contours as inside of their theoretical locations.

theoretical model of interpolated contour shape consisting of a constant-curvature arc tangential to the visible edges is generally consistent with the illusory

contour data of this experiment. Deviations from the model may be due to small individual differences in the perceived shapes of illusory contours or to response bias.<sup>7</sup>

Further examination of Fig. 10 suggested that observers perceived some contours to be in the correct location almost immediately, whereas other localizations changed substantially over time. Fig. 11 plots error in location, averaged across observers and collapsed across stimulus shape. By averaging across shape, this measure reflects, in part, the accuracy with which observers could distinguish between the corresponding fat and thin shapes. The accuracy with which observers localized real contours reached asymptote after 93.3 ms of processing. With illusory contours, observers required 120 ms of processing before accuracy of localization reached asymptote. These estimates correspond reasonably well with the estimates of when precision reached asymptote: 80 and 120 ms, respectively.

With the control stimuli, accuracy did not reach asymptote until an SOA of 173.3 ms. This estimate, which arose primarily from changes in responses to the fat shapes over time, deviates substantially from the estimate of 106.7 ms for reaching asymptotic precision. Below, we discuss possible explanations for this deviation.

#### 4.3. Discussion

At all tested durations, illusory contours produced more precise and accurate dot localization performance than control stimuli containing comparable spatial cues but no interpolated edges. This finding supports the notion that the dot localization paradigm, extended over time, probes emerging contour representations.

Illusory contour representations reached asymptotic precision after an estimated 120 ms of processing. As a comparison, perception of real contours reached maximal precision after 80 ms of processing. From these data, it appears that illusory contour formation lags the perception of luminance contours by about 40 ms. (With the later estimate of 93.3 ms for asymptotic accuracy of real contour perception, this difference shrinks to 26.7 ms; however, an inspection of Figs. 10 and 11 suggests that the accuracy of contour localization, though tech-

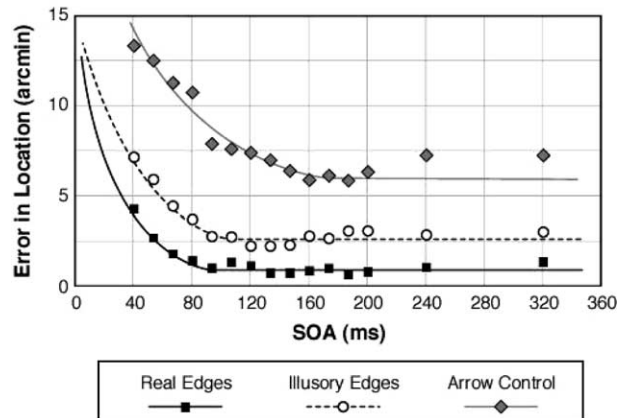


Fig. 11. Results of Experiment 3: Error in location as a function of SOA, averaged across observers. The lines represent the best fitting splines, calculated with the last two data points of each set omitted. Accuracy of real edge perception reached an asymptote of 0.9 arcmin at 93.3 ms of image processing. Localization accuracy of the illusory contours reached an asymptote of 2.5 arcmin after 120.0 ms of processing. Accuracy with the arrow controls reached an asymptote of 6.0 arcmin after 173.3 ms of processing.

nically not at asymptote, changed minimally between 80 and 93.3 ms.)

The 80 ms asymptote for real contours generally fits with an earlier estimate for contour integration time (Hess, Beaudot, & Mullen, 2001), despite using a different stimulus set and paradigm. Previous estimates of *interpolation* time were obtained from different methods and varied substantially with stimulus context (Guttman et al., 2003; Sekuler & Murray, 2001). Nonetheless, this estimate of 120 ms for contour completion seems rather short. Ringach and Shapley (1996), for example, estimated that local contour processing requires 117 ms, with global integration requiring an extra 140–200 ms. However, the shape classification technique giving rise to these estimates examined overall shape representations, rather than contour representations per se. Thus, Ringach and Shapley's suggested time course may include the duration for both contour interpolation and surface spreading (Grossberg & Mingolla, 1985; Yin, Kellman, & Shipley, 1997, 2000), with the latter prolonging the estimate. Alternatively, the contracted time course of the current experiment may have arisen from the nature of the stimulus presentation: Presenting the inducing circles prior to the illusory shape likely shortened the time required to process local edge information, as all but the inducing edges could be analyzed prior to stimulus presentation. Furthermore, the sudden appearance of an illusory shape in front of four complete circles leads to the perception of extremely strong interpolated contours (Lee & Nguyen, 2001), and strong contours may well develop more rapidly than weaker contours. With these considerations in mind, the estimate of 120 ms for contour interpolation seems reasonable.

<sup>7</sup> The "bias" explanation may be supported by the control data from observers FRJ and JLV. These two observers exhibited substantial difficulty with the fat but not the thin control stimuli. Post-experiment discussions with these observers suggested that this result may reflect the fact that the control stimuli were difficult to discriminate at short processing durations, and thus often led to a default "inside" response. The direction of these errors supports this hypothesis: The edges of the fat stimuli tended to be localized outside of their theoretical locations, and thus nearer to the boundaries of the thin stimuli.

With the stimuli containing illusory and real edges, accuracy and precision levels reached asymptote at similar durations. By contrast, these times diverged for the control stimuli. Observers achieved maximal precision within about 106.7 ms of stimulus onset, whereas maximal accuracy required significantly longer (173.3 ms). This finding may indicate the use of cognitive strategies: All necessary perceptual information may have been extracted from the inducers within 106.7 ms, although application of this information to the task—including the decision of whether the cues reflected a thin or fat shape—required significantly longer. In other words, though the basic perceptual information in the control stimuli did not vary over time, exposure duration may have affected the particular strategy used to infer “contour” location. Thus, after a relatively short duration (106.7 ms), precision varied little, but accuracy improved as a function of the different strategies available at different processing times.

Regardless of the reason for the deviation between the precision and accuracy measures, achieving optimal dot localization performance with the control stimuli took significantly longer than it did with the illusory stimuli. This finding further supports the idea that the dot localization task is sensitive to developing contour representations. Whereas the visual system processed illusory contour stimuli rapidly by interpolating perceptual representations between the visible contours, the control stimuli invited more prolonged cognitive processing.

## 5. General discussion

The study of perceptual organization is difficult, but also interesting, because perceptual representations go beyond the local characteristics of the stimulus. As critical information does not reside in the proximal stimulus, these representations cannot be addressed straightforwardly by signal detection methods. Thus, research in this area necessitates the development of paradigms that involve objective measurement yet can be reasonably interpreted as probing perceptual representations.

In the three experiments reported here, we investigated a novel dot localization paradigm for examining perceptual representations of interpolated contours. Our findings support the validity of the method and show how it may be used to further our knowledge about perceptual organization. Experiments 1 and 2 indicated that the visual system ultimately represents illusory and partly occluded contours with less precision and accuracy than luminance-defined contours, but with greater precision and accuracy than spatial-cue control stimuli, which index the level of performance that we might expect on the basis of cognitive strategies alone. These findings cohere with previous demonstrations that con-

tour interpolation involves basic perceptual mechanisms, rather than cognitive inference, spatial cueing, or recognition from partial information (e.g., Dresch & Bonnet, 1995; Gold et al., 2000; Peterhans & von der Heydt, 1989). Furthermore, the results of these experiments showed that straight contours typically lead to more precise and accurate dot localization performance than curved contours. In line with subjective report studies (Shipley & Kellman, 1992), this finding supports the notion that interpolation strength decreases with increasing contour curvature, as does the effectiveness with which real contour segments become integrated (Field et al., 1993).

Experiment 3 probed illusory contour representations at various times following stimulus onset. At all tested processing durations, as well as at asymptote, the precision and accuracy of illusory contour representations lagged those of the real contours, but exceeded those of the control stimuli. Importantly, the illusory contour stimuli showed a distinct microgenetic time course, with performance levels increasing systematically, but rapidly, with processing duration. The finding that completion takes measurable time previously has been demonstrated using perceptual classification techniques (Ringach & Shapley, 1996; Shore & Enns, 1997), priming methods (Guttman et al., 2003; Sekuler & Palmer, 1992), and visual search (Gegenfurtner et al., 1997; Rauschenberger & Yantis, 2001). In sum, the overall consistency of the current results with previous experiments establishes the dot localization paradigm as a valid and effective technique for the objective study of interpolated contour representations, both in their final states and as they emerge over time.

The claim of objectivity deserves some elaboration. Specifically, we suggest that our imprecision measure, though derived from subjective inside/outside judgments, represents an objective and intuitive metric for contour strength. Weaker contours or strategies for guessing will yield two effects: (1) greater variability across observers, and thus larger errors in location, on average; and (2) greater variability *within* observers, and thus lower precision. These correlated effects mean that accuracy and precision generally serve as converging measures of contour strength, as observed in the current study. However, the accuracy measure depends critically on the theoretical model to which one compares perceived contour locations, as well as any response biases relative to this model, and thus contains subjective components.

It is the observers' ability to be spatially consistent in their responses that yields essentially objective data about perceived contours. We suggest that consistency, as indexed by high precision, cannot be simulated by response bias. With control stimuli lacking interpolated contours, observers were markedly less precise and accurate, and showed a slower time course in their

improvement on these measures. Thus, the most parsimonious explanation for consistent, precise dot localization performance—particularly under speeded viewing conditions—is that the observer’s visual system represents a contour with some spatial precision, in a particular spatial location, and judges dot position relative to this representation. The precision of dot localization thus reflects the objective precision, or strength, of underlying contour representations. In measuring contour strength without relying on a subjective rating scale (e.g., Dumais & Bradley, 1976; Shipley & Kellman, 1990, 1992), the dot localization paradigm has the potential to elucidate several issues of contour interpolation, such as the extent to which spatial factors affect the completion process.

The dot localization paradigm may ultimately prove most useful, however, for examining the time course of contour interpolation. Previous techniques probing the microgenesis of illusory or partly occluded objects—including the primed-matching paradigm (Sekuler & Palmer, 1992), visual search with restricted presentation (e.g., Davis & Driver, 1998; Rauschenberger & Yantis, 2001), and shape classification (Ringach & Shapley, 1996)—confound the development of contour and surface representations. By contrast, the dot localization paradigm, when extended over time, focuses strictly on mapping the precision and accuracy of emerging contours.

This approach, utilized in Experiment 3, already has yielded some useful new information regarding the microgenesis of illusory contours. Importantly, contour interpolation—when considered independently of surface spreading (Grossberg & Mingolla, 1985; Yin et al., 1997, 2000)—can occur within the first 120 ms of visual processing, at least under optimal stimulus conditions. Further, the precision of illusory contour perception begins to improve well before real contour perception reaches maximal precision at around 80 ms, suggesting parallel processing of real and interpolated contours.

These findings may have implications for our understanding of the mechanisms underlying contour interpolation: Both results are highly consistent with network-style models of completion processes. Network models (e.g., Field et al., 1993; Yen & Finkel, 1998) characterize interpolation as an orientation-specific spread of activation through a network of laterally connected, collinear or co-circular units. As such, this low-level approach predicts both rapid interpolation and the emergence of all contour representations—luminance-defined and illusory—in parallel. Such predictions follow naturally from models utilizing higher-order operators (e.g., Heitger, von der Heydt, Peterhans, Rosenthaler, & Kübler, 1998): By a feed-forward approach, one might expect somewhat slower interpolation than observed, as well as a delay of longer than 40 ms relative to the processing of real edge information. As network-style and higher-order opera-

tor models also make different predictions regarding the influence of spatial factors on illusory contour microgenesis, additional experiments using the dot localization paradigm, currently underway (Guttman & Kellman, 2004), should further help to elucidate contour completion mechanisms.

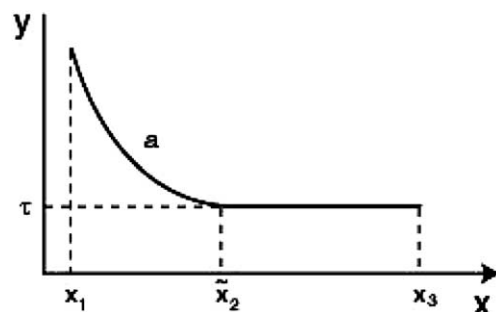
In sum, dot localization represents a useful technique for revealing the shape and precision of interpolated contours as they unfold over time. With certain patterns of data and appropriate control groups, the paradigm can serve as an essentially objective measure of perceptual organization. Current results using this approach suggest that illusory and partly occluded contours emerge through the processing of low-level mechanisms, rather than cognitive inference, over a shorter time course than previously believed. Further, the ultimate representations of interpolated contours decrease in strength with increasing curvature and deviate slightly from constant curvature paths. These findings may extend and elaborate geometric models of boundary completion (e.g., Kellman & Shipley, 1991). Future research using the dot localization paradigm should further enhance our understanding of the final representations, time courses, and ultimately the mechanisms underlying the interpolation of illusory and partly occluded contours.

## Acknowledgements

This work was presented at the 2002 meeting of the Vision Sciences Society, and forms part of the dissertation of SEG. The authors wish to thank John Hummel, Dario Ringach, Barbara Knowlton, Joaquin Fuster, Evan Palmer, Patrick Garrigan, Robert Hess, and an anonymous reviewer for helpful discussions, Tom Wickens and Alan Yuille for statistical consultation, and Jennifer Vanyo and Tony Raissian for general assistance. This work was supported by the National Eye Institute EY13518 to PJK and a Chancellor’s Dissertation Year Fellowship to SEG.

## Appendix A

*The spline:*



Model for curve fitting:

$$\begin{cases} y(x) = a(x - \tilde{x}_2)^2 + \tau & x_1 \leq x \leq \tilde{x}_2 \\ y(x) = \tau & x \geq \tilde{x}_2 \end{cases}$$

where  $x_1$  is the shortest tested image duration,  $\tilde{x}_2$  is the inflection point between the two segments of the spline,  $x_3$  is the longest tested image duration (see graph),  $a$  is the slope of the quadratic, and  $\tau$  is the value of the asymptote.

Energy of the model:

$$E[a, \tau, \tilde{x}_2] = \sum_{x=x_1}^{\tilde{x}_2-\Delta} (f(x) - a(x - \tilde{x}_2)^2 - \tau)^2 + \sum_{x=\tilde{x}_2}^{x_3} (f(x) - \tau)^2$$

where  $\Delta$  is the interval between tested image durations (13.33 ms).

Differentiating  $\frac{\partial}{\partial a}$  and minimizing:

$$0 = \sum_{x=x_1}^{\tilde{x}_2-\Delta} (f(x) - a(x - \tilde{x}_2)^2 - \tau)(x - \tilde{x}_2)^2$$

$$0 = \sum_{x=x_1}^{\tilde{x}_2-\Delta} (f(x) - a(x - \tilde{x}_2)^2 - \tau) + \sum_{x=\tilde{x}_2}^{x_3} (f(x) - \tau)$$

Solving for  $a$  and  $\tau$ :

$$\sum_{x=x_1}^{\tilde{x}_2-\Delta} f(x)(x - \tilde{x}_2)^2 = a \sum_{x=x_1}^{\tilde{x}_2-\Delta} (x - \tilde{x}_2)^4 + \tau \sum_{x=x_1}^{\tilde{x}_2-\Delta} (x - \tilde{x}_2)^2$$

$$\sum_{x=x_1}^{x_3} f(x) = a \sum_{x=x_1}^{\tilde{x}_2-\Delta} (x - \tilde{x}_2)^2 + \tau \sum_{x=x_1}^{x_3} 1$$

$$\begin{bmatrix} \sum_{x=x_1}^{\tilde{x}_2-\Delta} f(x)(x - \tilde{x}_2)^2 \\ \sum_{x=x_1}^{x_3} f(x) \end{bmatrix} = \begin{bmatrix} \sum_{x=x_1}^{\tilde{x}_2-\Delta} (x - \tilde{x}_2)^4 & \sum_{x=x_1}^{\tilde{x}_2-\Delta} (x - \tilde{x}_2)^2 \\ \sum_{x=x_1}^{\tilde{x}_2-\Delta} (x - \tilde{x}_2)^2 & \sum_{x=x_1}^{x_3} 1 \end{bmatrix} \begin{pmatrix} a \\ \tau \end{pmatrix}$$

Therefore:

$$\begin{pmatrix} a \\ \tau \end{pmatrix} = \frac{1}{D} \begin{pmatrix} \sum_{x=x_1}^{x_3} 1 & -\sum_{x=x_1}^{\tilde{x}_2-\Delta} (x - \tilde{x}_2)^2 \\ -\sum_{x=x_1}^{\tilde{x}_2-\Delta} (x - \tilde{x}_2)^2 & \sum_{x=x_1}^{\tilde{x}_2-\Delta} (x - \tilde{x}_2)^4 \end{pmatrix} \times \begin{pmatrix} \sum_{x=x_1}^{\tilde{x}_2-\Delta} f(x)(x - \tilde{x}_2)^2 \\ \sum_{x=x_1}^{x_3} f(x) \end{pmatrix}$$

$$a = \frac{1}{D} \left[ \left( \sum_{x=x_1}^{x_3} 1 \right) \left( \sum_{x=x_1}^{\tilde{x}_2-\Delta} f(x)(x - \tilde{x}_2)^2 \right) - \left( \sum_{x=x_1}^{x_3} f(x) \right) \left( \sum_{x=x_1}^{\tilde{x}_2-\Delta} (x - \tilde{x}_2)^2 \right) \right]$$

$$\tau = \frac{1}{D} \left[ - \left( \sum_{x=x_1}^{\tilde{x}_2-\Delta} (x - \tilde{x}_2)^2 \right) \left( \sum_{x=x_1}^{\tilde{x}_2-\Delta} f(x)(x - \tilde{x}_2)^2 \right) + \left( \sum_{x=x_1}^{x_3} f(x) \right) \left( \sum_{x=x_1}^{\tilde{x}_2-\Delta} (x - \tilde{x}_2)^4 \right) \right]$$

where  $D = \left( \sum_{x=x_1}^{\tilde{x}_2-\Delta} (x - \tilde{x}_2)^4 \right) \left( \sum_{x=x_1}^{x_3} 1 \right) - \left( \sum_{x=x_1}^{\tilde{x}_2-\Delta} (x - \tilde{x}_2)^2 \right)^2$ .

Solving for the energy of the model:

$$E[a, \tau, \tilde{x}_2] = \sum_{x=x_1}^{\tilde{x}_2-\Delta} f(x) (f(x) - a(x - \tilde{x}_2)^2 - \tau) + \sum_{x=\tilde{x}_2}^{x_3} f(x)(f(x) - \tau)$$

$$= \sum_{x=x_1}^{x_3} (f(x))^2 - a \sum_{x=x_1}^{\tilde{x}_2-\Delta} f(x)(x - \tilde{x}_2)^2 - \tau \sum_{x=x_1}^{x_3} f(x)$$

$$= \sum_{x=x_1}^{x_3} (f(x))^2 + g(\tilde{x}_2)$$

where

$$g(\tilde{x}_2) = \frac{1}{D} \begin{bmatrix} - \left( \sum_{x=x_1}^{x_3} 1 \right) \left( \sum_{x=x_1}^{\tilde{x}_2-\Delta} f(x)(x - \tilde{x}_2)^2 \right)^2 \\ + 2 \left( \sum_{x=x_1}^{\tilde{x}_2-\Delta} (x - \tilde{x}_2)^2 \right) \left( \sum_{x=x_1}^{x_3} f(x) \right) \\ \times \left( \sum_{x=x_1}^{\tilde{x}_2-\Delta} f(x)(x - \tilde{x}_2)^2 \right) \\ - \left( \sum_{x=x_1}^{\tilde{x}_2-\Delta} (x - \tilde{x}_2)^4 \right) \left( \sum_{x=x_1}^{x_3} f(x) \right)^2 \end{bmatrix}$$

To determine the best-fitting spline, the energy of the model was calculated for each possible value of  $\tilde{x}_2$ . The  $\tilde{x}_2$  leading to the lowest energy was defined as the duration at which the curve reached asymptote, then was substituted into the appropriate equations to determine the best-fitting  $a$  and  $\tau$ .

References

Davis, G., & Driver, J. (1998). Kanizsa subjective figures can act as occluding surfaces at parallel stages of visual search. *Journal of Experimental Psychology: Human Perception and Performance*, 24, 169–184.

Derman, C. (1957). Non-parametric up-and-down experimentation. *Annals of Mathematical Statistics*, 28, 795–797.

- Dresp, B., & Bonnet, C. (1991). Psychophysical evidence for low-level processing of illusory contours and surfaces in the Kanizsa square. *Vision Research*, *31*, 1813–1817.
- Dresp, B., & Bonnet, C. (1993). Psychophysical measures of illusory form perception: Further evidence for local mechanisms. *Vision Research*, *33*, 759–766.
- Dresp, B., & Bonnet, C. (1995). Subthreshold summation with illusory contours. *Vision Research*, *37*, 913–924.
- Dumais, S. T., & Bradley, D. R. (1976). The effects of illumination level and retinal size on the apparent strength of subjective contours. *Perception & Psychophysics*, *19*, 339–345.
- Falmagne, J. C. (1986). Psychophysical measurement and theory. In K. R. Boff, L. Kaufman, & J. P. Thomas (Eds.), *Handbook of perception and human performance. Vol. 1. Sensory processes and perception* (pp. 1–66). New York: John Wiley & Sons.
- Fantoni, C., & Gerbino, W. (2003). Good continuation by vector-field combination. *Journal of Vision*, *3*, 281–303.
- Field, D. J., Hayes, A., & Hess, R. F. (1993). Contour integration by the human visual system: Evidence for a local “association field”. *Vision Research*, *33*, 173–193.
- Gegenfurtner, K. R., Brown, J. E., & Rieger, J. (1997). Interpolation processes in the perception of real and illusory contours. *Perception*, *26*, 1445–1458.
- Gold, J. M., Murray, R. F., Bennett, P. J., & Sekuler, A. B. (2000). Deriving behavioural receptive fields for visually completed contours. *Current Biology*, *10*, 663–666.
- Greene, H. H., & Brown, J. M. (1997). Spatial interactions with real and gap-induced illusory lines in vernier acuity. *Vision Research*, *37*, 597–604.
- Gregory, R. L. (1972). Cognitive contours. *Nature*, *238*, 51–52.
- Grossberg, S., & Mingolla, E. (1985). Neural dynamics of form perception: Boundary completion, illusory figures, and neon color spreading. *Psychological Review*, *92*, 173–211.
- Guttman, S. E., & Kellman, P. J. (2004). Mechanisms of contour interpolation: Evidence from a dot localization paradigm, in press.
- Guttman, S. E., Sekuler, A. B., & Kellman, P. J. (2003). Temporal variations in visual completion: A reflection of spatial limits? *Journal of Experimental Psychology: Human Perception and Performance*, *29*, 1211–1227.
- Heitger, F., von der Heydt, R., Peterhans, E., Rosenthaler, L., & Kübler, O. (1998). Simulation of neural contour mechanisms: Representing anomalous contours. *Image and Vision Computing*, *16*, 407–421.
- Hess, R. F., Beaudot, W. H. A., & Mullen, K. T. (2001). Dynamics of contour integration. *Vision Research*, *41*, 1023–1037.
- Hunt, S. M. J. (1994). MacProbe: A Macintosh-based experimenter’s workstation for the cognitive sciences. *Behavior Research Methods, Instruments, and Computers*, *26*, 351–356.
- Kanizsa, G. (1976). Subjective contours. *Scientific American*, *234*, 48–52.
- Kellman, P. J., Guttman, S. E., & Wickens, T. D. (2001). Geometric and neural models of object perception. In T. F. Shipley & P. J. Kellman (Eds.), *From fragments to objects: Segmentation and grouping in vision* (pp. 183–245). New York: Elsevier.
- Kellman, P. J., & Shipley, T. F. (1991). A theory of visual interpolation in object perception. *Cognitive Psychology*, *23*, 141–221.
- Kellman, P. J., Shipley, T. F., & Kim, J. (1996). Global and local effects in object completion: Evidence from a boundary localization paradigm. *Abstracts of the Psychonomic Society*, *1*, 34.
- Kellman, P. J., Temesvary, A., Palmer, E. M., & Shipley, T. F. (2000). Separating local and global processes in object perception: Evidence from an edge localization paradigm. *Investigative Ophthalmology and Visual Science*, *41*(4), 741.
- Kellman, P. J., Yin, C., & Shipley, T. F. (1998). A common mechanism for illusory and occluded object completion. *Journal of Experimental Psychology: Human Perception and Performance*, *24*, 859–869.
- Lee, T. S., & Nguyen, M. (2001). Dynamics of subjective contour formation in the early visual cortex. *Proceedings of the National Academy of Sciences*, *98*, 1907–1911.
- McCourt, M. E., & Paulson, K. (1994). The influence of illusory contours on the detection of luminance increments and decrements. *Vision Research*, *34*, 2469–2475.
- Murray, R. F., Sekuler, A. B., & Bennett, P. J. (2001). Time course of amodal completion revealed by a shape discrimination task. *Psychonomic Bulletin & Review*, *8*, 713–720.
- Peterhans, E., & von der Heydt, R. (1989). Mechanisms of contour perception in monkey visual cortex. II. Contours bridging gaps. *Journal of Neuroscience*, *9*, 1749–1763.
- Pillow, J., & Rubin, N. (2002). Perception completion across the vertical meridian and the role of early visual cortex. *Neuron*, *33*, 805–813.
- Pomerantz, J. R., Goldberg, D. M., Golder, P. S., & Tetewsky, S. (1981). Subjective contours can facilitate performance in a reaction time task. *Perception & Psychophysics*, *29*, 605–611.
- Rauschenberger, R., & Yantis, S. (2001). Masking unveils pre-amodal completion representation in visual search. *Nature*, *410*, 369–372.
- Ringach, D. L., & Shapley, R. (1996). Spatial and temporal properties of illusory contours and amodal boundary completion. *Vision Research*, *36*, 3037–3050.
- Rubin, N. (2001). The role of junctions in surface completion and contour matching. *Perception*, *30*, 339–366.
- Schoumans, N., & Sittig, A. C. (2000). Illusory contours and spatial judgment. *Perception & Psychophysics*, *62*, 1191–1203.
- Sekuler, A. B., & Murray, R. F. (2001). Amodal completion: A case study in grouping. In T. F. Shipley & P. J. Kellman (Eds.), *From fragments to objects: Segmentation and grouping in vision* (pp. 265–294). New York: Elsevier.
- Sekuler, A. B., & Palmer, S. E. (1992). Perception of partly occluded objects: A microgenetic analysis. *Journal of Experimental Psychology: General*, *121*, 95–111.
- Shipley, T. F., & Kellman, P. J. (1990). The role of discontinuities in the perception of subjective contours. *Perception & Psychophysics*, *48*, 259–270.
- Shipley, T. F., & Kellman, P. J. (1992). Perception of partly occluded objects and illusory figures: Evidence for an identity hypothesis. *Journal of Experimental Psychology: Human Perception and Performance*, *18*, 106–120.
- Shore, D. I., & Enns, J. T. (1997). Shape completion time depends on the size of the occluded region. *Journal of Experimental Psychology: Human Perception and Performance*, *23*, 980–998.
- Takeichi, H. (1995). The effect of curvature on visual interpolation. *Perception*, *24*, 1011–1020.
- Tse, P. U., & Albert, M. K. (1998). Amodal completion in the absence of image tangent discontinuities. *Perception*, *27*, 455–464.
- Ullman, S. (1976). Filling in the gaps: The shape of subjective contours and a model for their generation. *Biological Cybernetics*, *25*, 1–6.
- Yen, S. C., & Finkel, L. H. (1998). Extraction of perceptually salient contours by striate cortical networks. *Vision Research*, *38*, 719–741.
- Yin, C., Kellman, P. J., & Shipley, T. F. (1997). Surface completion complements boundary interpolation in the visual integration of partly occluded objects. *Perception*, *26*, 1459–1479.
- Yin, C., Kellman, P. J., & Shipley, T. F. (2000). Surface integration influences depth discrimination. *Vision Research*, *40*, 1969–1978.